Final Showcases (D2.4 - SGA3)

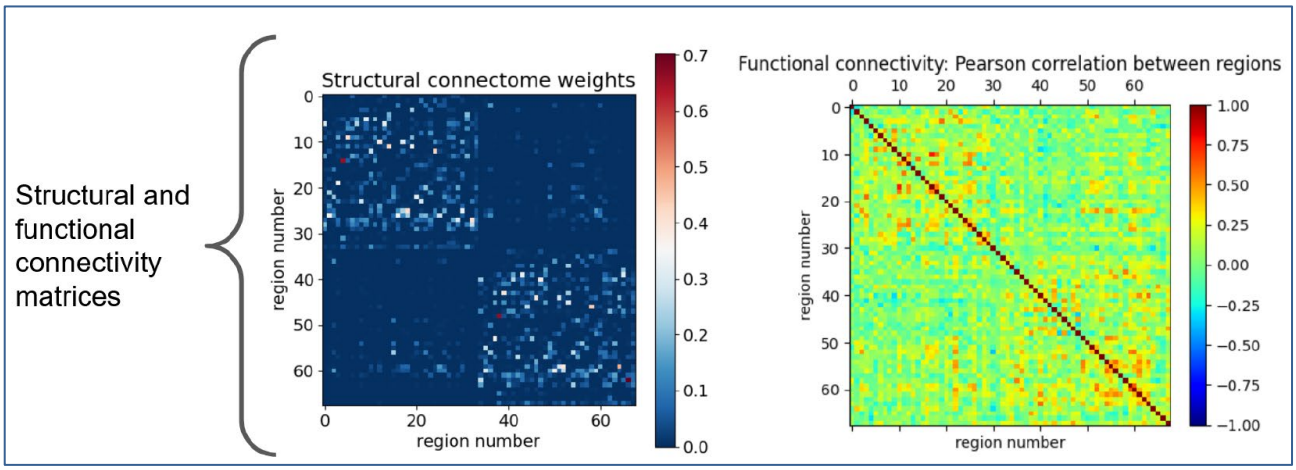

Figure 1: Structural connectivity (SC, left) and functional connectivity (FC, right) matrices.

The correlation between FC and SC varies with states of consciousness during simulated slow waves and this can be captured by whole-brain models as shown below.

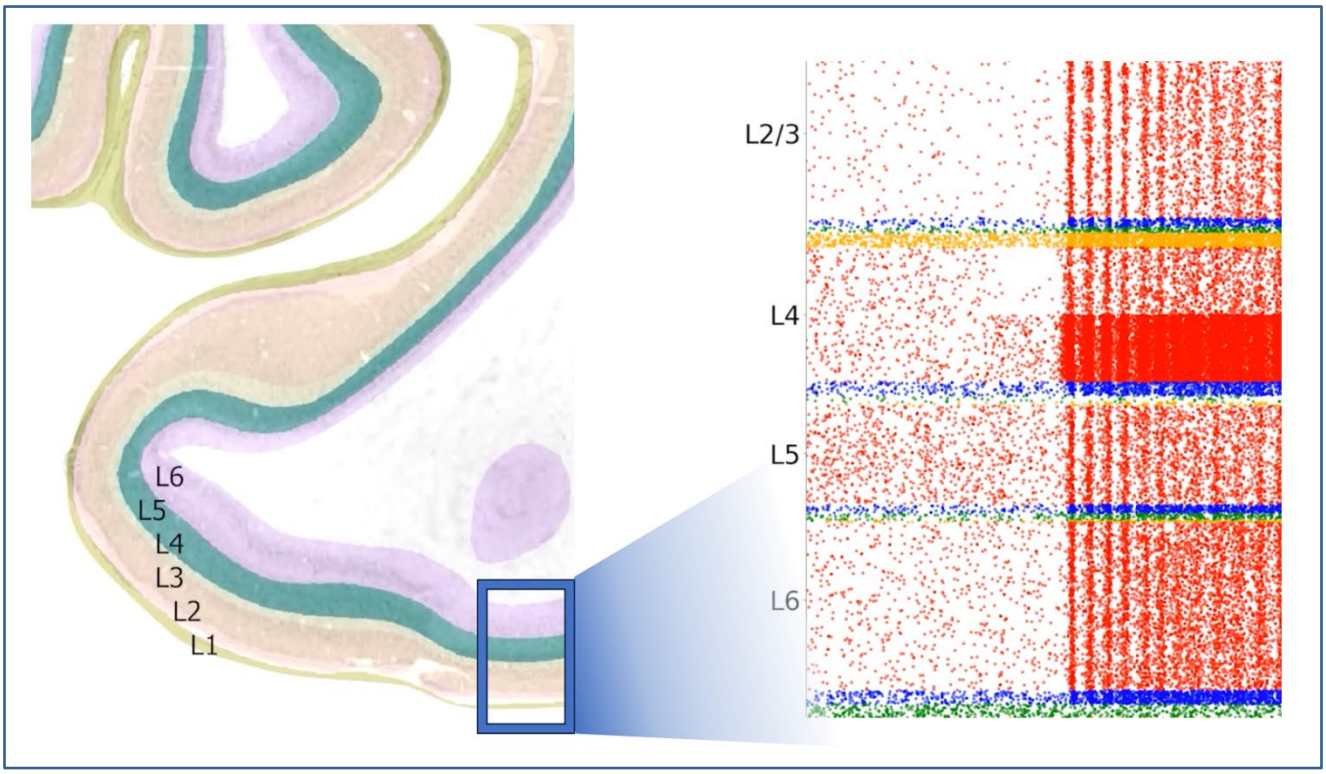

Figure 2: A computational model of primary visual cortex reflects detailed neural dynamics

Left: slice of the human primary visual cortex, showing the different cortical layers in different colours. Right: time-dependent activity of all cortical layers and cell types for a small section of the visual cortex, as simulated by our computational model. Each dot indicates a spike from a pyramidal (red), PV (blue), SST (green) and VIP (yellow) cell in the computational model. Halfway through the simulation, an external current is injected into the network leading to the emergence of oscillatory activity.

Project Number:	945539	Project Title:	HBP SGA3

Document Title:	Final Showcases (D2.4 – SGA3)
Document Filename:	D2.4 (D15) SGA3 M42 SUBMITTED 230911.docx
Deliverable Number:	SGA3 D2.4 (D15)
Deliverable Type:	**Demonstrator:** DEM: Demonstrator, pilot, prototype, plan designs
Dissemination Level:	PU = Public
Planned Delivery Date:	SGA3 M42 / 30 SEP 2023
Actual Delivery Date:	SGA3 M42 / 11 SEP 2023
Author(s):	Alain DESTEXHE, CNRS (P10), Cyriel PENNARTZ, UVA (P98)
Compiled by:	Angelica DA SILVA LANTYER, UVA (P98)
Contributor(s):	Alain DESTEXHE, CNRS (P10), contributed to Section 1 Maria Sacha, CNRS (P10), contributed to Section 1.2.1 Rodrigo Cofre, CNRS (P10), contributed to Section 1.2.2 Elodie Leveque, CNRS (P10), contributed to Section 1.2.2 Jorge MEJIAS, UVA (P98), contributed to Section 2 Umberto OLCESE, UVA (P98) contributed to Section 2.2 Eric DIJKEMA, UVA (P98) contributed to Section 2.2 Giulia MORENI, UVA (P98) contributed to Section 2.3 Kwangjun LEE, UVA (P98) contributed to Section 2.4 Matthias BRUCKLACHER, UVA (P98) contributed to Section 2.5
WP QC Review:	Arnau MANASANCH, IDIBAPS (P93)
WP Leader / Deputy Leader Sign Off:	Mavi SANCHEZ-VIVES, IDIBAPS (P93)
T7.4 QC Review:	N/A
Description in GA:	Showcase 3 – DEMO3.3 Full brain simulation corresponding to different brain states and consciousness levels integrating meso and microcortical mechanisms. Showcase 4 – DEMO4.3 Simulation of object and scene recognition v3. This simulation will illustrate how the brain may achieve image and scene recognition through the process of learning to construct internal models (latent representations) of objects and the environment. In addition, the demonstration will document which data have been gathered and curated to inform the model, how the data are used to build models, object perception recognition in large-scale networks, and how data and model applications can unfold for neuromorphic computing and robotics
Abstract:	This new demo of Showcase 3 depicts first a model of anaesthesia, where the action of anaesthetics has been explicitly considered in the model. We have integrated the action of anaesthetics such as propofol, isoflurane, sevoflurane or barbiturates on the GABA-A receptor, or the action of anaesthetics such as ketamine or xenon on the NMDA receptor in the mean-field models. This was implemented in TVB to yield models where the action on synaptic receptors can be evaluated at the large-scale

	(whole brain). The model obtained was checked using PCI measurements or FC-SC correlation measures, against data on human and monkey. Beyond the interest of studying states of consciousness, this model constitutes a very useful tool to evaluate the emerging consequences at large scales resulting from changes at the molecular level (synaptic receptors). The new demo of Showcase 4 describes the computational models of perception and predictive coding across scales. As such it also shows how the computational bridging of neural dynamics models and models of perception and cognition can be accomplished. We first demonstrate a detailed and realistic cortical column network, including pyramidal cells and four types of interneurons in each cortical layer, in which we introduce synaptic plasticity, giving rise to biologically observed patterns of rhythmic oscillations. Using these principles, we next show how a cortical column model performs predictive coding, based on interneuron-pyramidal cell circuits (a hybrid of dynamic and cognitive modelling). Next, we proceed to show how predictive coding can be used to compute view-invariant object representations and object segmentation based on self- versus external object motion. Altogether, these multi-scale models reveal a unique approach to combine neurobiological realism with perceptual-cognitive task performance.
Keywords:	Computational models, states of consciousness, anaesthesia, whole-brain, predictive coding, object recognition, perception.
Target Users/Readers:	Computational neuroscience community, computer scientists, consortium members, public, neuroinformaticians, neuroscientific community, neuroscientists, platform users, policymakers, researchers, scientific community, students.

Table of Contents

Table of Figures

1. Showcase 3: Brain Complexity and Consciousness, Demo 3

1.1 Introduction

In the last years, modelling work in HBP has focused on reproducing different brain states, gradually moving from circuits to the whole brain. In SGA1, we started from the level of spiking neurons, and in particular networks of excitatory and inhibitory neurons, and determined the conditions by which such Adaptive Exponential (AdEx) networks can generate different states, such as asynchronous-irregular (AI) or slow-wave oscillatory (Up-Down) states (Zerlaut et al., 2018; di Volo et al., 2019). Such spiking network models were compared to experimental data at cellular resolution, such as typically unit recordings with microelectrodes.

In SGA2, we moved to the population level by constructing mean-field models of AdEx networks. The AdEx mean-field model could successfully reproduce the population-level transitions between AI and Up/Down states found in spiking networks (di Volo et al., 2019). Because they are much faster to simulate, mean-field models could be scaled up to larger brain areas at the millimetre scale ("mesoscale"), typically modelling one brain area. This is done by constructing networks of mean-field models, that can be constrained from imaging data (for example, from voltage-sensitive dye imaging of monkey visual cortex – see Zerlaut et al., 2018).

To scale up to larger scales, in SGA3 we have integrated the AdEx mean-field models into The Virtual Brain (TVB) simulator, to yield the so-called TVB-AdEx model (Goldman et al., 2022). This model simulates large networks of mean-field models, connected according to the connectome. The TVB-AdEx model is a multi-scale approach where information about the biophysical properties of neural networks is directly used to build and compute the dynamics at large scales. The information gained at the mesoscale is also used to build the TVB-AdEx model. This model was shown to reproduce the spontaneous activity during two states, the asynchronous dynamics of wakefulness and the synchronized slow-wave dynamics of sleep. Most importantly, the model could reproduce experimental observations of a diminished responsiveness and information spread in slow-wave sleep compared to wakefulness (Goldman et al., 2022), as observed experimentally (Massimini et al. 2005). Finally, in the Showcase 3 Demo 3.2[1], we have shown that this approach can be used to model not only the human brain, but also mouse and monkey brains. In particular, the precise imaging that can be done in mice is a very efficient way to constrain the mouse TVB-AdEx model (Tort-Colet et al., in preparation).

In Demo 3.3, we take a step back to the cellular/synaptic level, by modelling anaesthetics using known mechanisms of their action on synaptic receptors and use the TVB-AdEx model to evaluate its emerging consequences at the large-scale level in the brain. These consequences include spontaneous activity, responsiveness, and how the dynamics relate to the connectome.

1.2 Technical Specification

1.2.1 TVB-AdEx model of general anaesthesia

1.2.1.1 Anaesthesia acts on synaptic receptors

In the previous demos of Showcase 3, general anaesthesia was modelled by changing the parameter of spike-frequency adaptation to higher levels than the one used to model slow-wave sleep (SWS).

[1] https://www.humanbrainproject.eu/en/follow-hbp/news/2022/06/20/how-ebrains-used-investigate-disorders-consciousness/

In demo 3.3, we are following a different approach that considers the effect of the common general anaesthetics on synaptic receptors.

At the molecular level, general anaesthetics alter neuronal behaviour through their interactions with ion channels on the postsynaptic membrane that result in a change of the neuronal excitability. Generally, these drugs exert their action either by decreasing excitatory or enhancing inhibitory signals. This results from their effect on two main postsynaptic receptors (Hemmings et al., 2005): a first family of anaesthetics act as agonists of the $GABA_A$ receptor, a chloride ion channel receptor of γ-aminobutyric acid (GABA), the main inhibitory neurotransmitter in the central neural system (CNS). This is the case for propofol, isoflurane, sevoflurane, or barbiturates. A second family of anaesthetics act as antagonist of NMDA receptors, a non-selective cationic channel, the ligand of which is glutamate, the main excitatory neurotransmitter in the CNS. This is the case for anaesthetics such as ketamine or xenon, which primarily act as NMDA-blockers. Thus, the effect of these interactions leads to either decreased excitatory or enhanced inhibitory synaptic transmission, resulting in a global decrease of excitability.

To account for these synaptic phenomena and develop a biologically relevant model for anaesthesia, we considered the effect of two parameters in the AdEx model, the excitatory (τe) and inhibitory (τi) synaptic decay. We are modelling the effect of the NMDA-blockers by decreasing the value of the excitatory synaptic decay (τe), resulting in a faster decay of the excitatory synaptic currents, which translates to a shorter excitatory action. In a similar manner, the effect of $GABA_A$ agonists will be modelled by increasing the value of τi.

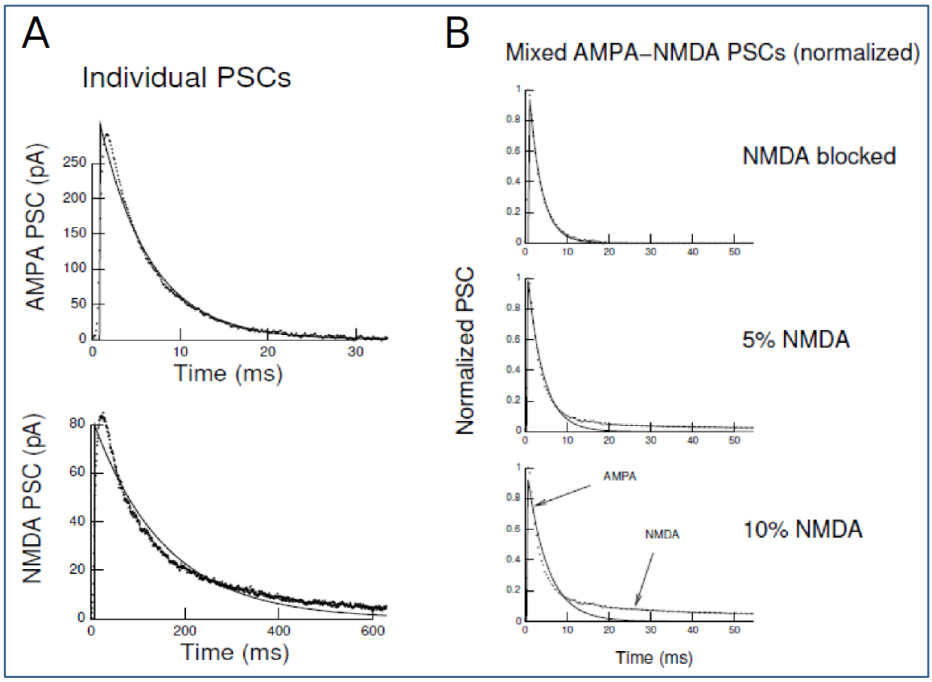

Figure 3: Biophysical simulation of the effect of anaesthetics on glutamate receptors.

A. Fits to individual postsynaptic currents (PSCs; AMPA on top, NMDA bottom). B. Simulation of mixed AMPA-NMDA PSCs, and their respective fit with a single exponential decay. The fitted value had a decay time constant of 3, 4 and 5 ms, respectively, from top to bottom.

Figure 3 shows a biophysical simulation to illustrate how the antagonism of NMDA receptors leads to a shortening of the kinetics of the conductance of AMPA/NMDA excitatory synaptic input. When the NMDA receptors are partially or completely blocked, as seen under the influence of ketamine, the time constant indeed decreases as compared to the scenario when the NMDA receptors remain largely intact (at approximately 10% functionality), where the time constant extends to approximately 5 milliseconds. Notably, the impact on amplitude is rather minimal, primarily because the dominant contribution to the maximal current amplitude comes from the AMPA current. As a result, we can disregard the influence of ketamine on the quantal conductance of the excitatory synaptic input in the model.

Similar findings have been reported for the $GABA_A$ agonism (reviewed in Hemmings et al., 2005): the action of agonists such as barbiturates or propofol has been shown in patch-clamp experiments to

slow-down the decay of the $GABA_A$ current, with no measurable effect on amplitude. Thus, in this case as well, the action of anaesthetics on $GABA_A$ receptors can be modelled by a change of the decay time of the synaptic current in the model.

1.2.1.2 Spontaneous activity

We used the TVB-AdEx model published recently (Goldman et al., 2022) to simulate these actions of anaesthetics on synaptic receptors.

Figure 4 shows the dynamics of the TVB-AdEx model following these changes of synaptic receptors. One can see that in the case of NMDA antagonists (Fig. 3A), the shortening of tau_e can lead to a transition from asynchronous (wake-like) activity to synchronized slow-wave (anaesthesia-like) activity in the whole brain model. The same transition can be observed when prolonging the time constant of inhibition, mimicking the effect of GABA agonists (Fig. 3B). Thus, the TVB-AdEx model can produce the emergence of slow-wave activity, solely by changing the value of the tau_e and tau_i parameters:

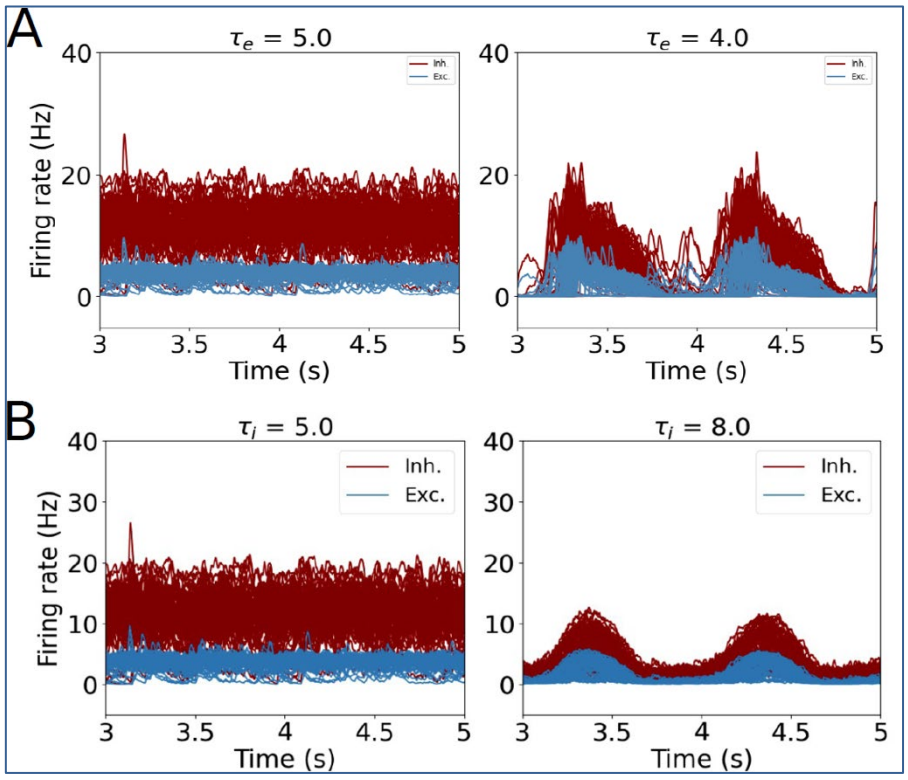

Figure 4: Simulation of the effect of anaesthetics on synaptic receptors in the TVB-AdEx model.

A. Transition from asynchronous (left) to slow-wave (right) activities by antagonizing NMDA receptors. B. Similar transition obtained by agonists of GABA-A receptors.

1.2.1.3 Evoked activity and responsiveness

A more severe test of the model is to attempt to reproduce the experimental measurements of responsiveness to external stimuli. The main experimental observation was that the responsiveness, as measured by the Perturbational Complexity Index (PCI), markedly dropped during anaesthesia with loss of consciousness (Casali et al., 2013). This was found for both $GABA_A$ and NMDA related anaesthetics, with no significant differences between the PCI values of the different unconscious states (Massimini et al., 2005; Casali et al., 2013). In Figure 5 we show that in the case of unconscious states, that are modeled either by increasing the value of spiking frequency adaptation (b_e) in the case of simulated SWS, or by changing the synaptic decays for anaesthesia-like conditions, the

propagation of the brain response to perturbation is less complex when compared to the asynchronous wake-like state, expressed with lower PCI values.

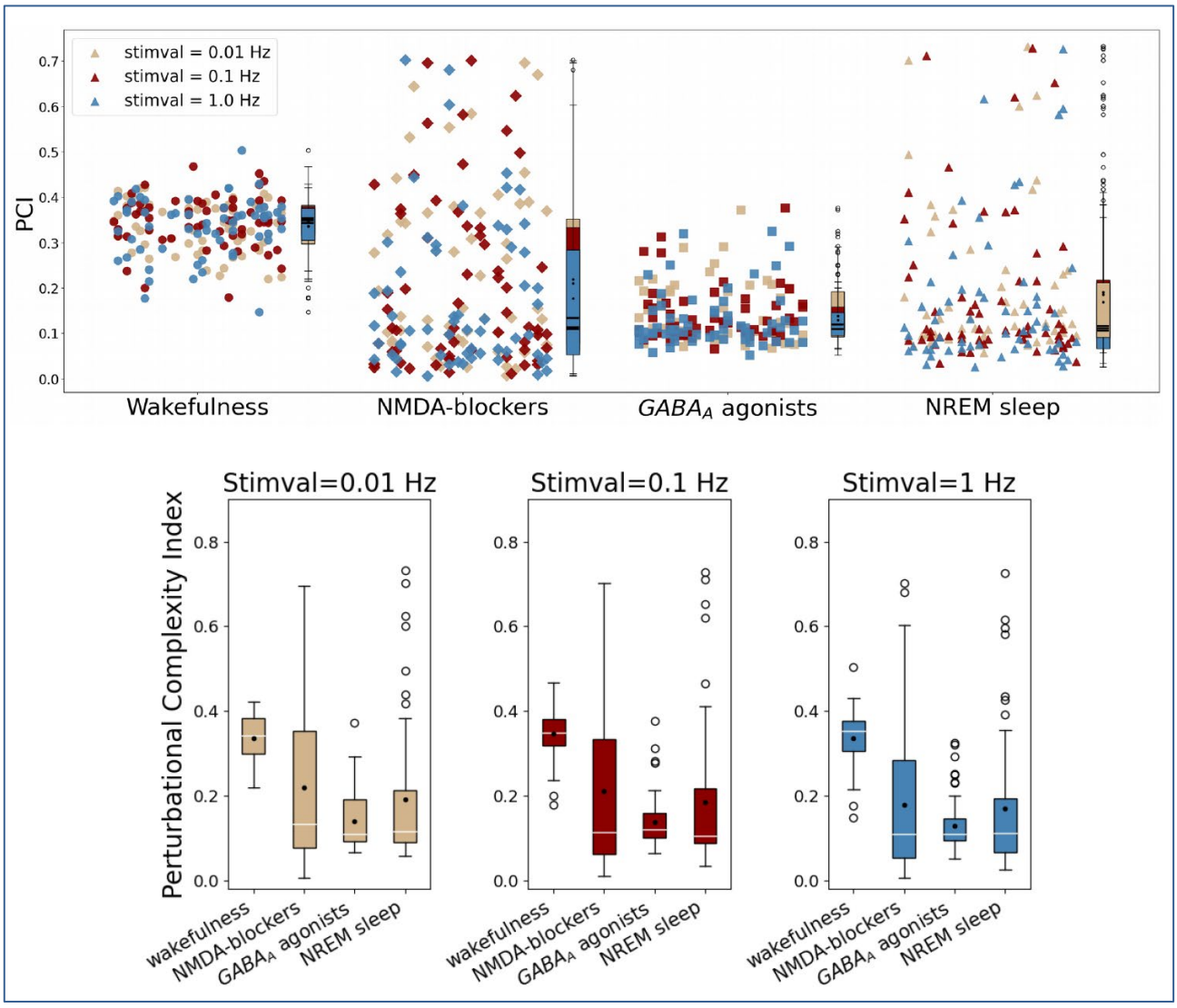

Figure 5: PCI values for the cases of wakefulness, anaesthesia (NMDA-blockers and GABAA receptors) and NREM sleep.

On the scatterplot on top, we show the PCI values for 60 different realisations of simulations for each of the states of consciousness, when applying a stimulus of different intensities. To assess the statistical significance of the difference between the conditions, post-hoc Conover tests were performed, adjusted using the Holm-Bonferroni method to control for multiple comparisons (where ***: p<0.001). Interestingly no significant differences were found between the different unconscious states, in accordance with the empirical data.

1.2.2 Correlation between functional and structural connectivity in human, monkey, and models

We used the TVB-AdEx model published recently (Goldman et al., 2022) and extended to simulate the effect of propofol anaesthesia (see Section 1.2.1) to investigate the functional connectivity of the model, compared to human and monkey data.

The human data consisted of an ensemble of 48 scans from 16 subjects who were recorded by fMRI, and for which the connectome was available (Naci et al. 2018). The data is openly available in OpenNeuro (Kandeepan et al., 2020). From these data, we computed the functional connectivity (FC) using Pearson correlation methods applied to the fMRI data. The FC was compared to the structural connectivity (SC) given by the connectome. The correlation between the FC map and the SC map was computed for each subject and the results are shown in Fig. 6 (left), showing a significant increase of the FC-SC correlation during anaesthesia.

The same paradigm was simulated using the TVB-AdEx model for propofol anaesthesia (measured as in Figure 1). Functional connectivity (FC) was calculated using Pearson's cross-correlation. As in the data, the model exhibited a higher FC-SC correlation during slow-waves (Fig. 6, right).

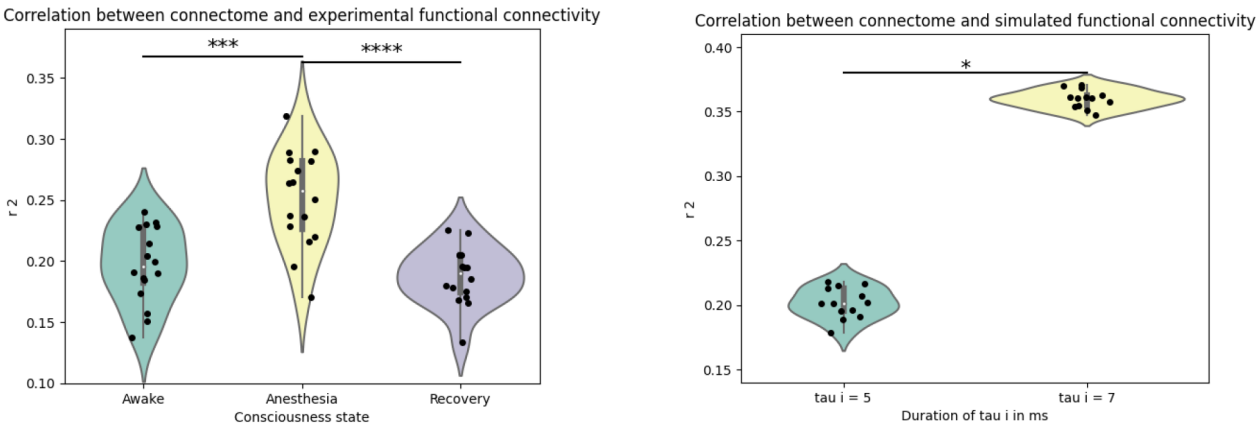

Figure 6: Violin plots showing the correlation between the structural connectivity and the functional connectivity.

Left: experimental data, 48 human subjects divided in the three 16-subject-groups: awake, anaesthesia and recovery. r2: Pearson correlation factor. ***p < 0.001, ****p < 0.0001. ANOVA test followed by Student tests. Right: simulations using the TVB-AdEx model. 32 simulations performed with different noises and divided in the two 16-subject-groups: τi = 5 ms and τi = 7 ms. *p < 0.05. Student test.

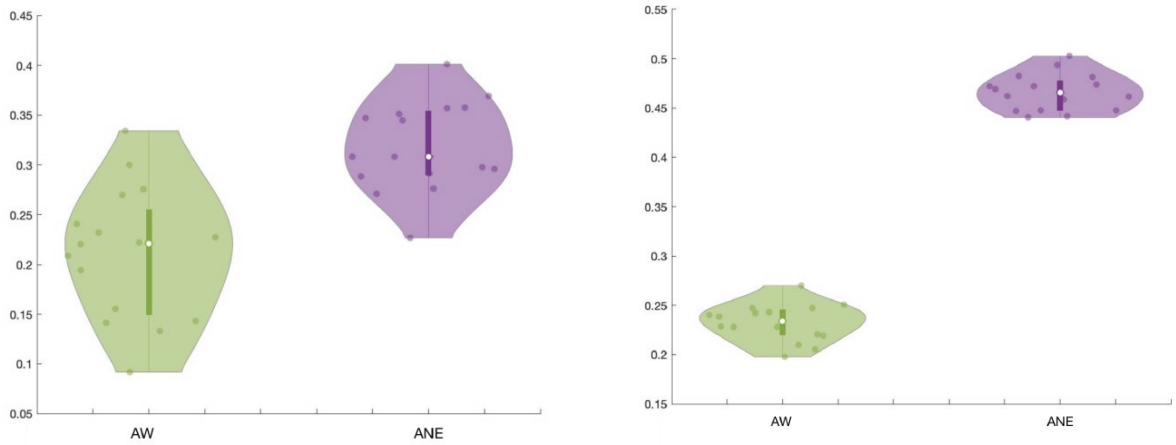

Left: 16 macaques recorded in fMRI in awake (AW) and anesthetized (ANE) conditions, showed an increase of the SC-

Figure 7: Correlation between functional connectivity and structural connectivity in awake and anesthetized macaques, as well as in the TVB-AdEx model.

FC correlation during anesthesia. Right: same paradigm simulated with the TVB-AdEx macaque model, where propofol anesthesia was simulated by a slow-down of $GABA_A$ receptors.

The same analysis was performed for macaques. Here, we used a dataset kindly provided by Bechir Jarraya from NeuroSpin (Tasserie et al., 2022). The data consisted of 16 macaques recorded in fMRI and for which the connectome was measured using tractography. The monkeys were recorded while awake and after anaesthesia with propofol. As for the human subjects, the correlation FC-SC was higher during anaesthesia (Fig. 6, left). The TVB-AdEx model was used to replicate these experimental conditions, using the macaque connectome (see Showcase 3 demo 3.2[2]). The simulated asynchronous activity and slow-wave activity mimicking propofol also produced the same effect: the correlation FC-SC was higher in slow-wave states (Fig. 6, right).

2 https://www.humanbrainproject.eu/en/follow-hbp/news/2022/06/20/how-ebrains-used-investigate-disorders-consciousness/

Thus, in the real and simulated brains, and for both human and monkey, the asynchronous dynamics associated to conscious wakefulness generates patterns of activity which significantly depart from the patterns that would be predicted by connectivity. In other words, the activity patterns generated in conscious states are richer than during anaesthesia, where the activity is well predicted by the physical connectivity. Although slow waves are more synchronized across the brain, and display higher values of FC, their spatial organization remains close to the connectome, so in these unconscious states, the patterns of activity are more predictable from the knowledge of the connectome.

1.3 How to access the showcase

Model of anaesthesia: https://wiki.ebrains.eu/bin/view/Collabs/showcase-3-tvb-brain-states-modelling/Drive?srid=4KtuLIKu#Anesthesia.

1.4 Conclusions and future directions

This work has succeeded to model the two main types of anaesthetic actions, leading to the emergence of slow-wave activity typical of anaesthesia, and reproducing key properties of anesthetized states. Thus, we think the TVB-AdEx model constitutes a powerful tool for evaluating the emergent properties of brain activity, or changes of brain activity, due to changes at the level of synaptic receptors or membrane conductance. The same approach could be used to study brain pathologies, and how alterations at the molecular level can lead to changes at the brain scale. Similarly, the effect of drugs (other than anaesthetics) could be studied using the TVB-AdEx model.

There is presently no other way to estimate the global emergent consequences of molecular actions, and we hope the TVB-AdEx constitutes a useful tool to investigate these multi-scale interactions.

1.5 References

Casali AG, Gosseries O, Rosanova M, Boly M, Sarasso S, Casali KR, Casarotto S, Bruno MA, Laureys S, Tononi G, Massimini M. A theoretically based index of consciousness independent of sensory processing and behavior. Sci Transl Med. 2013 Aug 14;5(198):198ra105. doi: 10.1126/scitranslmed.3006294. PMID: 23946194

P1864: Di Volo M, Romagnoni A, Capone C and Destexhe A. (2019) Biologically realistic mean-field models of conductance-based networks of spiking neurons with adaptation. *Neural Computation* 31: 653-680. doi: https://doi.org/10.1162/neco_a_01173.

P3023: Goldman JS, Kusch L, Hazal Yalcinkaya B, Depannemaecker D, Nghiem TA, Jirsa V and Destexhe A. (2022) A comprehensive neural simulation of slow-wave sleep and highly responsive wakefulness dynamics. *Frontiers in Computational Neuroscience* 16: 1058957. DOI: https://doi.org/10.3389/fncom.2022.1058957

P4144: Jennifer S. Goldman, Maria Sacha, Lionel Kusch, and Alain Destexhe. (2023) Asynchronous and slow-wave oscillatory states in connectome-based models of mouse, monkey, and human cerebral cortex. Biorxiv: https://www.biorxiv.org/content/10.1101/2023.08.03.551869v1

DOI: https://doi.org/10.1101/2023.08.03.551869

Hemmings, H. C. *et al*. (2005) Emerging molecular mechanisms of general anaesthetic action. *Trends Pharmacol. Sci.* **26**, 503–510.

Kandeepan S, Rudas J, Gomez F, Stojanoski B, Valluri S, Owen AM, Naci L, Soddu A and Nichols ES. (2020) Using anesthesia-induced loss of consciousness to identify biomarkers of conscious awareness in the healthy human brain. Open Neuro Dataset https://openneuro.org/datasets/ds003171/versions/1.0.0 DOI: 10.18112/openneuro.ds003171.v1.0.0

Massimini, M. *etal*. (2005) Break down of cortical effective connectivity during sleep. *Science* **309**, 2228–2232.

Naci, L., Haugg, A., MacDonald, A., Anello, M., Houldin, E., Naqshbandi, S., Gonzalez-Lara, L. E., Arango, M., Harle, C., Cusack, R., & Owen, A. M. (2018). Functional diversity of brain networks supports consciousness and verbal intelligence. *Scientific Reports*, 8(1), 1–15. https://doi.org/10.1038/s41598-018-31525-z

Tasserie J, Uhrig L, Sitt JD, Masanova D, Dupont M, Dehaene S and Jarraya B. (2022) Deep brain stimulation of the thalamus restores signatures of consciousness in a nonhuman primate model. *Science Advances* 8: eabl5547. DOI: https://doi.org/10.1126/sciadv.abl5547

P1019: Zerlaut, Y., Chemla, S., Chavane, F. and Destexhe, A. (2018) Modeling mesoscopic cortical dynamics using a mean-field model of conductance-based networks of adaptive exponential integrate-and-fire neurons. J. Computational Neurosci. 44: 45-61.

2. Showcase 4: Perception and Recognition of Objects and Scenes, Demo 4.3

2.1 Introduction

For the third and final demonstrator of Showcase 4, Demo 4.3, our goal was to finalize several computational descriptions of predictive coding models of perception, which cover both neurobiological and cognitive aspects. More specifically, Showcase 4 has progressed towards three computational models which incorporate different levels of biological realism: 1) a neurobiological model, which simulates a realistic spiking cortical column using available connectivity data from the literature and the Knowledge Graph; 2) a neurobiological-cognitive hybrid model, which depending of the version is constructed with a biologically realistic neuron model (i.e. spiking neuron) or a differentiated cellular circuitry (i.e. PV-SST-VIP circuits) and a local learning rule (i.e. Hebbian learning) to perform object reconstruction; and 3) a cognitive model, which is built with rate-based neurons to focus on extending the cognitive ability of the hybrid model by introducing movement invariance and visuomotor corrections. The knowledge gained from the three models will improve our understanding of perception and sensory predictions, offer valuable insights in neural mechanisms of brain disorders such as autism or schizophrenia, and inspire neuromorphic, artificial intelligence and robotic applications.

The models explained below make use of and contribute to the EBRAINS Research Infrastructure (RI) in several ways. The neurobiological model uses anatomical data from the Knowledge Graph and other external datasets, such as the Allen Institute for Brain Science, to estimate the connection strengths and probabilities derived from mouse visual cortex. It also uses a Simulation service tool, ViSimpl, to visualise the spatial and temporal features of spiking cortical columns. The hybrid model also uses Community service of the EBRAINS Research Infrastructure (RI). Given our successful application for FENIX computing and storage resources, the hybrid and cognitive models have been trained to generate internal representations of visual input on a supercomputer (CSCS Piz Daint). In collaboration with the Scientific Liaison Unit (SLU), we have also implemented the hybrid model on the EBRAINS RI and add it to the list of Simulation service models (CWL). With intuitive GUIs, novice users are now able to run example simulations with a pre-trained version of the hybrid model. Advanced users or researchers in relevant fields can conduct sustainable simulations using the embedded model and compare their results with other models listed in the Simulation service.

The insight provided by these models will be useful for other uses beyond computational modelling of perception. Given the generative nature of both cognitive and hybrid models, they have the potential for a wide range of downstream applications that can benefit from efficient learning of sensory inputs (e.g., AI, prostheses, robotics, etc.). The local learning of connection weights and the asynchronous, event-driven activities of the spiking hybrid model can also contribute to the development of energy-efficient neuromorphic computing.

2.2 Technical Specification

The following section is divided into three subsections, each of which corresponds to one of the three computational models we developed and provides technical details. At this stage, the three models have converged towards a common conceptual framework, which is reflected in the fact that models now share fundamental properties –such as the presence of multiple cell types across the neurobiological and hybrid models, the representational capacities in the hybrid and cognitive models, and the Hebbian-like learning rules in all models.

2.2.1 Neurobiological model of a cortical column

Our first attempt to understand predictive coding in a neurobiological setting starts with understanding the functioning of the biological constituents of cortical columns, given that they

seem to form the fundamental blocks of prediction error circuits and therefore predictive coding (Attinger et al., 2017, Hertag et al. 2020). To this aim, we built a computational model of a cortical column in the visual cortex.

The model incorporates pyramidal cell circuits plus three different interneuron types (PV, SST and VIP cells) and the dynamic properties of AMPA, GABA and NMDA receptors. Data about the cellular properties of each cell type (including capacitance values, firing thresholds, etc), as well as the cell-specific and laminar-specific mean synaptic strength and connection probabilities, have been constrained by existing anatomical and electrophysiological data. The first version of the model was entirely built in NEST, a powerful simulator for spiking neural network models, to allow for a quick prototyping of the core dynamics of the model. Part of the simulations to understand the dynamics of the cortical column were also performed using this tool. Then using ViSimpl we were able to develop a 3D visualisation of the column showing the level of activity of the different neuron types. The resulting model matched in vivo cell type-specific firing rates for spontaneous and stimulus-evoked conditions in mice (Figure 8), although rhythmic activity was absent.

Interestingly, upon introduction of long-term spike-timing dependent plasticity and after driving the model with external sensory input, the columnar model developed broad-band (15-50 Hz) oscillatory dynamics, with frequency and power defined by the sensory input as observed in previous experimental studies. Although neural rhythms are ubiquitous in cortical recordings, this constitutes an important finding because it is unclear whether they emerge due to the basic structure of cortical microcircuits or depend on function. In the cortical model, synaptic plasticity was a prerequisite for the emergence of oscillations, which suggests a link between experience-dependent structures and rhythmic activity. Rhythms relied on all cell types, and oscillatory activity was linked to the plasticity-triggered fine structural motifs. Therefore, our results suggest that (i) rather than simply emerging from the structure of naïve columnar circuits in rodent V1, the emergence of neural rhythms in visual cortical columns might require of fine structural changes elicited by learning-related mechanisms, and (ii) the interactions between different cell types are important to understand the functioning of visual cortex.

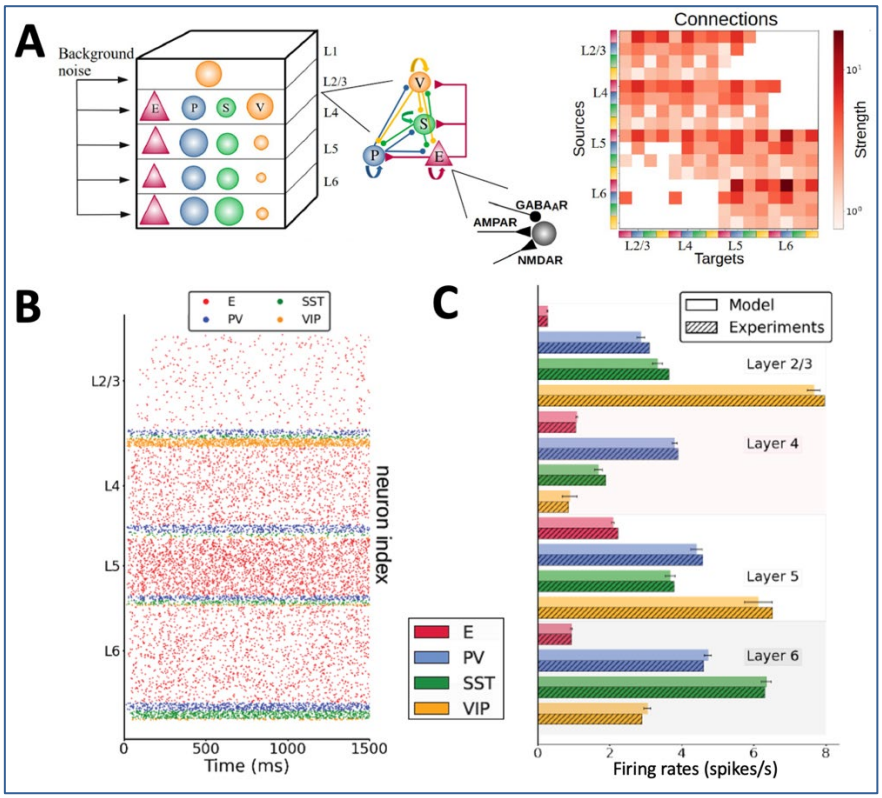

Figure 8: V1 cortical column model

(A) Scheme of the V1 cortical column model, displaying the laminar structure, cell types, circuitry, and synaptic receptor types. The averaged connectivity strength per layer and cell type is shown in the matrix on the right (source: Allen Institute). (B) Raster plot showing the spontaneous activity of the model for different layers and cell types. (C) Comparison between model predictions and experimental data. Bars display mean values plus/minus SEM.

2.2.2 Hybrid neurobiological-cognitive models

Our next step was to incorporate some of the relevant biological elements of the model above into a simplified model of predictive coding. In the context used here, a hybrid model is a mathematical description which contains and successfully merges ingredients from both realistic, neurobiological models and more abstract but cognitively powerful models. The hybrid model presented here has two variants: one focused on implementing spiking computations, and the other one involving multiple cell types.

While predictive coding is an influential theory in the field of neuroscience, its biological plausibility is yet to be proven. In our first version of a hybrid model, denoted as Spiking neural network for predictive coding (SNN-PC), we showed that predictive coding can be implemented on a neural network model with biologically plausible mechanisms of synaptic transmission and plasticity using spiking neurons (Figure 9; P3898). To accommodate the binary, pulsatile behaviour of spiking neurons, we separated the error neuron in classic predictive coding models (Rao & Ballard, 1999) into positive and negative units and developed a NMDA-receptor-mediated learning rule that approximate Hebbian learning. Moreover, the slow recurrent process of predictive coding was complemented by the fast feedforward gist signalling pathway, which models the feedforward sweep, to account for a comprehensive picture of visual processing.

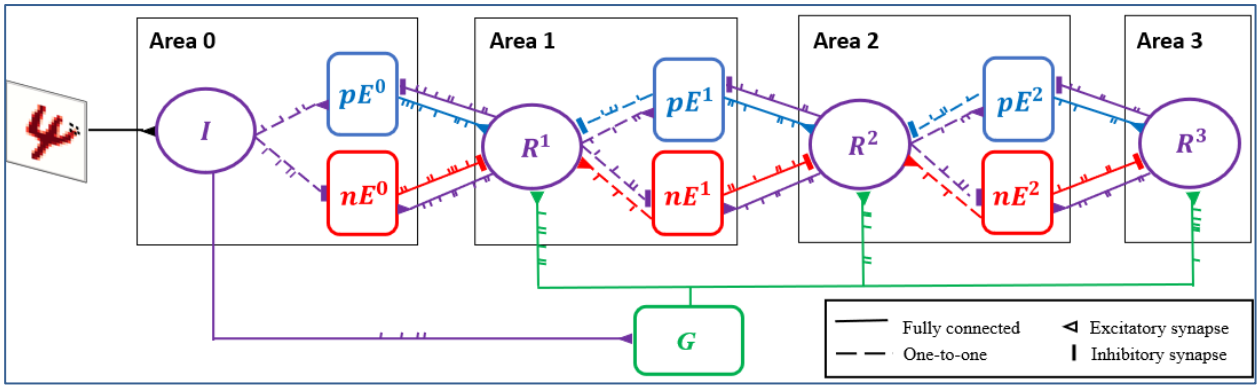

Figure 9: Spiking neural network for predictive coding (SNN-PC)

SNN-PC modeling the first stages of the visual cortical processing hierarchy. The three areas roughly correspond to V1, V2, and V4, respectively (or LGN, V1, and V2). Each non-input area (l > 0) consists of a representation unit (purple circle; R^l) and two units (blue and red squares; pE^l and nE^l) that encode positive and negative prediction error, respectively. The representation unit in Area 0 acts as an input unit (R^0). Each pixel (the dotted box in the image of digit 4) is encoded by a single spiking neuron. Note that each unit consists of multiple spiking neurons. The feedforward gist pathway (l→G→R^l) approximates the feedforward sweep of neuronal activity across the visual processing hierarchy. The solid lines between units indicate that they are fully connected, whereas the dotted lines indicate one-to-one connections. A triangle represents an excitatory synapse, whereas a thick vertical short ending represents an inhibitory synapse.

To further investigate the compatibility of the predictive coding theory with the brain, we developed another model (CoCo-PC; Figure 10) that introduce a rich diversity of neuron types and consistent column structures across the cortical hierarchy. We first conducted an exhaustive search through combinations of synaptic connections into (i.e., bottom-up and top-down inputs) and within (i.e., between neuron types) a microcircuit that consists of four major neuron types (pyramidal, PV, SST, and VIP) to identify microcircuit structures capable of prediction error computation (Attinger et al, 2017; Hertag et al. 2020). Then, we connected the identified microcircuits to facilitate predictive coding of visual inputs, while reflecting the anatomical projections and laminar organizations in the cortex. Our model not only proposes a possible neural implementation of predictive coding in the cortex but also makes experimentally testable predictions on the role of each neuron type in predictive coding during perceptual inference and learning.

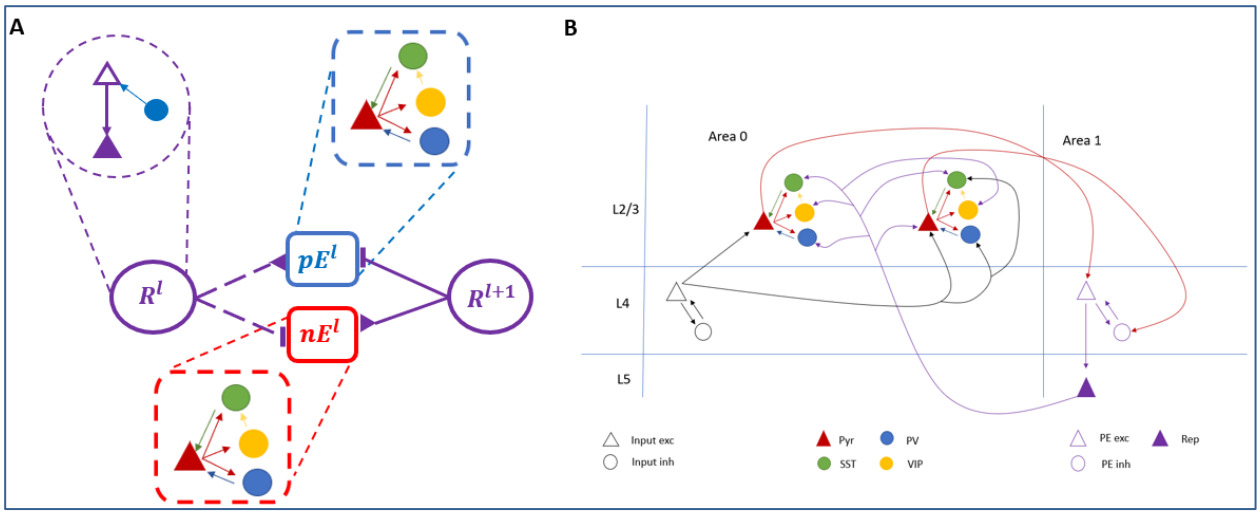

Figure 10: Cortical column model of predictive coding (CoCo-PC).

Cortical column model of predictive coding (CoCo-PC). A. Expanding single neuron models into microcircuit models. Representation neuron (R) is replaced by a microcircuit with two pyramidal cells and one PV cell. Prediction error neurons (pE and nE) are replaced by microcircuits with a pyramidal cell and three interneurons (PV, SST, and VIP). The superscript (l) represents an area in the cortical hierarchy. B. Predictive coding with biologically plausible cell type diversity, laminar organizations, and anatomical projections. Each row represents a cortical column (e.g., layer 2/3, 4, and 5). Each column represents an area in the visual cortex (e.g., V1 and V2). K. Lee et al., in prep.

2.2.3 Cognitive model for object recognition

Finally, we developed and implemented a set of cognitive models aimed at characterizing the complex computations underlying high-level perceptual properties of the visual ventral stream. The ventral pathway needs to fulfil at least two key functions: perceived objects must be mapped to high-level representations invariantly of the precise viewing conditions, and a generative model must be learned that allows, for instance, to fill in occluded information guided by visual experience. We showed how a multi-layered predictive coding network, based on the same principles of the hybrid model above (but with reduced biological properties) can learn to recognize objects from the bottom up and to generate specific view-invariant-representations via a top-down pathway through a single learning rule: the local minimization of prediction errors (Brucklacher et al. 2022). Trained on sequences of continuously transformed objects, neurons in the highest network area became tuned to object identity invariant of precise position, comparable to inferotemporal neurons in macaques (Figure 11). Drawing on this, the dynamic properties of invariant object representations reproduced experimentally observed hierarchies of timescales from low to high levels of the ventral processing stream. The predicted faster decorrelation of error-neuron activity compared to representation neurons is of relevance for the experimental search for neural correlates of prediction errors. Lastly, the generative capacity of the network was confirmed by reconstructing specific object images, robust to partial occlusion of the inputs. By learning invariance within a generative model, despite little change in architecture and learning rule compared to static input- reconstructing Hebbian predictive coding networks, simply by shifting the training paradigm to dynamic inputs, the approach generalizes the predictive coding framework to dynamic inputs in a more biologically plausible way than self-supervised networks with non-local error-backpropagation.

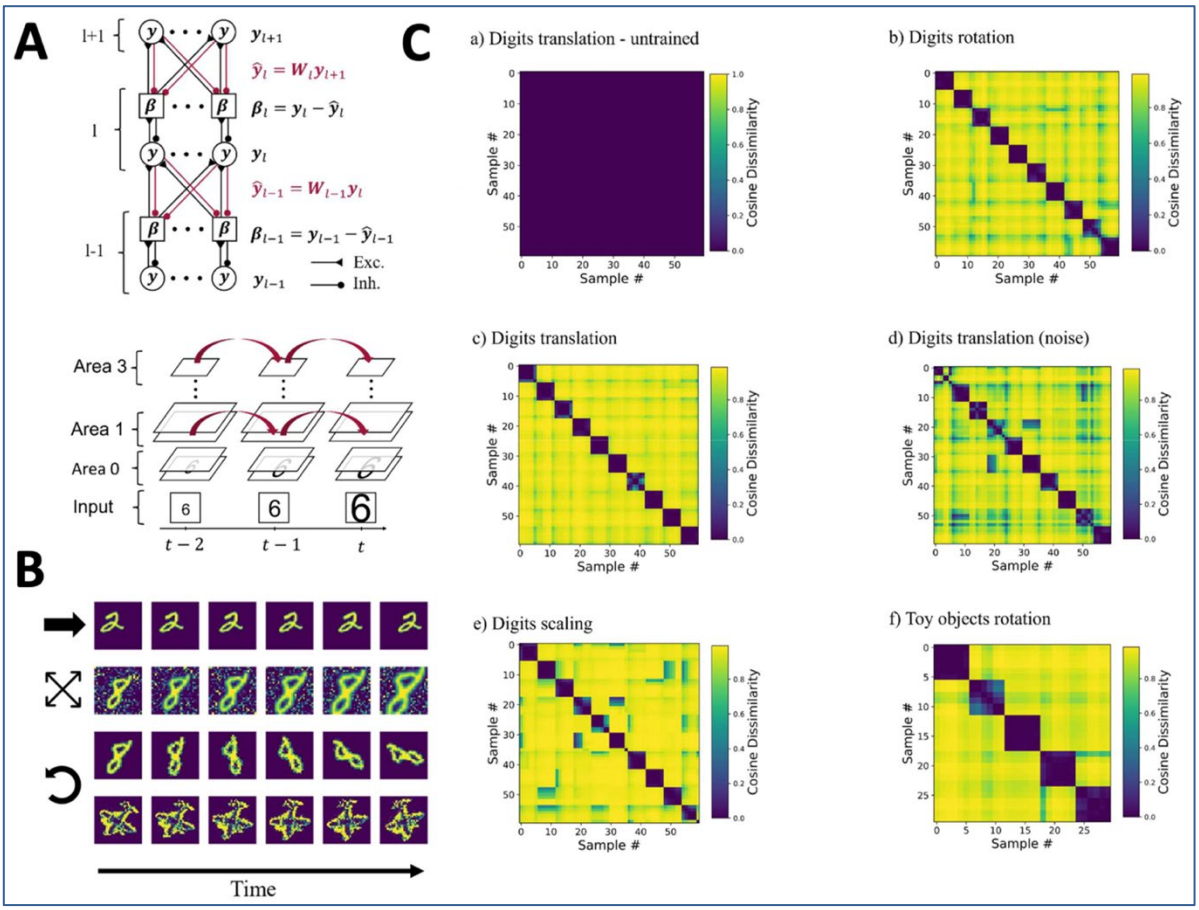

Figure 11: Neurons in the highest network area became tuned to object identification

(A) Scheme of the model (top) and processing of scaling input across areas and time (bottom). (B) Input sets with translational, scaling, and rotational properties. (C) Representational dissimilarity matrices for all cases in B -the low dissimilarity values in the diagonal terms show that representations for the same category are most related to stimuli in the same category. This indicates a good categorization performance, and top-down inputs will then provide category-specific information to facilitate the recognition of bottom-up signals. From: Brucklacher et al. (in press) (+biorxiv, PLUS-number).

A second important question in understanding sensory processing is how the brain differentiates self- from externally generated visual signals. In natural behaviour, this becomes important when recognizing a moving predator during locomotion: on the retina, the image of both background (such as trees in a forest) and predator move. To determine which is which, it is assumed that the brain learns to suppress irrelevant information. In this case these are the self-generated components of the optic flow. Based on evidence of sensorimotor mismatch in rodents (Zmarz et al. 2016, Attinger et al. 2017) we constructed a generative model of optic flow processing shown in Figure 12. The model naturally extends our previous work on predictive coding of moving inputs (Brucklacher et al. 2022) that is available in the EBRAINS Knowledge Graph by considering locomotion. The core component of the extended model is a microcircuit from motor to early visual areas shown to the right of Figure 12. Here, error neurons in primary visual cortex (V1) compare predictions about self-generated optic flow to the true sensory input. Deviations from expectations are used to drive learning with a Hebbian learning rule. Responses in this population reproduce observed mismatch responses from (2) as well as experience-dependence thereof. Remaining prediction errors are then fed forward to a purely visual area processing extended patches of optic flow. Due to the correspondence of these characteristics to middle temporal cortex, the model area is termed MT. After training on objects moving independently in front of a background, we find that predictions from this area segment out external causes, i.e., solve the problem of determining the external object of interest (‘predator’). Furthermore, class identity can be read out with decent accuracy from population activity in line with observed mild shape tuning of primate area MT in structure-from-motion experiments (Andersen et al. 1996). To conclude, the model offers a unification of several hallmarks of visual processing (segmentation, classification) and observed neural responses (sensorimotor mismatch) under the predictive coding framework.

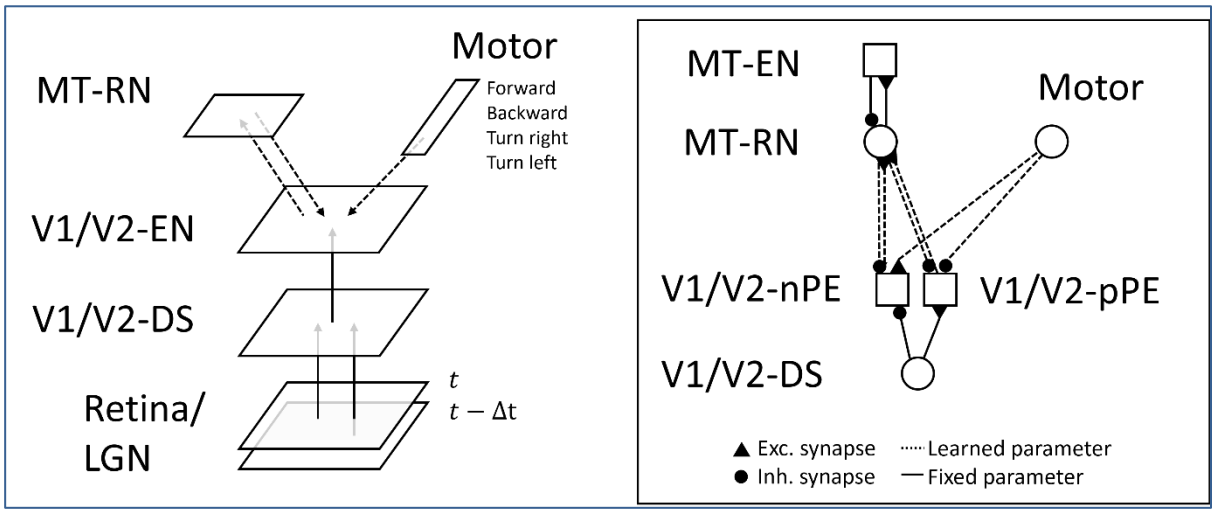

Figure 12: Generative model of optic flow processing

Left: hierarchical, multi-area generative model of optic flow and mapping onto brain areas. Right: the neural circuitry of the model. Squares denote error neurons while circles denote representation neurons. Brucklacher et al. (in prep.).

2.3 How to access the showcase

2.3.1 Showcase 4 Demo video

The Showcase 4 Output is a video entitled: **The dynamic cortex in perception and learning** (**https://www.youtube.com/watch?v=yr1bho_iTv4**), which has been published at the HBP YouTube Channel, that introduces the motivation and background of our research and summarises the three models (2.2.1, 2.2.2 and 2.2.3) at a level that can be understood by both lay audiences and scientific communities.

2.3.2 Access to code for the models

The previous, relevant work on predictive coding neural networks (Dora et al., 2021) and robotics implementations (Knowles et al., 2021) of our work have been published and can be accessed via the following link: https://search.kg.ebrains.eu/instances/10d36794-7177-4521-9e45-3943d96c776c.

The deep neural network model for predictive coding with Hebbian learning (Dora et al., 2021) has been published and can be accessed via the following link (soon to be incorporated to EBRAINS): https://github.com/shirindora/DGHPC

The code for the neurobiological cortical column model has been submitted to EBRAINS and is under curation.

The code for the hybrid model has been uploaded to EBRAINS and is under curation. The pretrained CWL implementation can be accessed here: https://gitlab.ebrains.eu/technical-coordination/project-internal/standardised-workflows/sc4_cwl

The code for the cognitive model is available here: https://search.kg.ebrains.eu/instances/0b219bf1-dead-4a06-811a-fdce66f2ec7d.

2.4 Conclusions and future directions

The work presented in this section displays a major advance in the development of computational models (and their underlying theoretical frameworks) which aim for both biologically detailed

descriptions and cognitive/computational capabilities. With common elements transversing across multiple modelling levels, such as spiking dynamics, cell-type variability, neuroanatomical structure, stable neural representations, invariant object recognition and sensorimotor integration, these models point towards to a new generation of computational descriptions focused on an attractive convergence between dynamics and function. Future directions include the reinforcement of connections between these models (for example, implementing predictive coding principles in a network of biologically detailed cortical column models), but also a progression towards models which include information about brain states, as they are likely to influence perception and the effectiveness of predictive coding paradigms. The hybrid model presented in 2.2.2 – while already presenting a combination of neural dynamics with generative modelling of sensory representations - is a natural candidate for further convergence, given its central position in terms of biological plausibility and computational capabilities.

2.5 References

Andersen RA, Bradley DC, Shenoy KV, Neural Mechanisms for Heading and Structure-from-Motion Perception, Cold Spring Harb Symp Quant Biol, 61:15–25, 1996.

Attinger A, Wang B, Keller GB, Visuomotor Coupling Shapes the Functional Development of Mouse Visual Cortex, Cell, 169(7):1291-1302.e14, 2017.

P3919: Brucklacher M, Bohte SM, Mejias JF, Pennartz CMA, Local minimization of prediction errors drives learning of invariant object representations in a generative network model of visual perception, bioRxiv, p. 2022.07.18.500392, 2022.

L Hertäg, H Sprekeler, Learning prediction error neurons in a canonical interneuron circuit, eLife 9, e57541, 2020.

RPN Rao, DH Ballard, Predictive coding in the visual cortex: a functional interpretation of some extra-classical receptive-field effects, Nature neuroscience 2 (1), 79, 1999.

Zmarz P, Keller GB. Mismatch receptive fields in mouse visual cortex, Neuron, 92(4):766–72, 2016.

P4133: Moreni, G, Pennartz, C. M. A., Mejias. (2023) J. F. Synaptic plasticity is required for oscillations in a V1 cortical column model with multiple interneuron types; bioRxiv 2023.08.27.555009; doi: https://doi.org/10.1101/2023.08.27.555009. This article is a preprint and has not been certified by peer review.

P3898: Lee K, Dora S, Mejias JF, Bohte SM, Pennartz CMA (2023) Predictive coding with spiking neurons and feedforward gist signalling. BioRxiv https://doi.org/10.1101/2023.04.03.535317